An intra-cytoplasmic route for SARS-CoV-2 transmission unveiled by Helium-ion microscopy

Antonio Merolli (antonio.merolli@gmail.com)
Rutgers University https://orcid.org/0000-0001-5704-2066
Leila Kasaei
Rutgers University
Santhamani Ramsamy
Rutgers University
Afsal Kolloli
Rutgers, The State University of New Jersey
Ranjeet Kumar
Rutgers, The State University of New Jersey
Selvakumar Subbian
Rutgers, The State University of New Jersey https://orcid.org/0000-0003-2021-8632
Leonard Feldman
Rutgers University

Article

Keywords: SARS-CoV-2, Helium-ion microscopy, Tunneling Nano Tubes, Cell fusion, Extracellular Vesicles, Transmission, Infection

Posted Date: October 20th, 2021

DOI: https://doi.org/10.21203/rs.3.rs-967568/v1

Abstract

SARS-CoV-2 virions enter the host cells by docking their spike glycoproteins to the membrane-bound Angiotensin Converting Enzyme 2. After intracellular assembly, the newly formed virions are released from the infected cells to propagate the infection, using the extra-cytoplasmic ACE2 docking mechanism. However, the molecular events underpinning SARS-CoV-2 transmission between host cells are not fully understood. Here, we report the findings of a scanning Helium-ion microscopy study performed on Vero E6 cells infected with mNeonGreen-expressing SARS-CoV-2. Our data reveal, with unprecedented resolution, the presence of: 1)-long tunneling nanotubes that connect two or more host cells over submillimeter distances; 2)-large scale multiple cell fusion events (syncytia); and 3)-abundant extracellular vesicles of various sizes. Taken together, these ultrastructural features describe a novel intra-cytoplasmic connection among SARS-CoV-2 infected cells that may act as an alternative route of viral transmission, disengaged from the well-known extra-cytoplasmic ACE2 docking mechanism. Our findings may explain the elusiveness of SARS-CoV-2 to survive from the immune surveillance of the infected host.

1. Introduction

In the well-documented route of SARS-CoV-2 infection of the upper respiratory tract, virions contained in airborne droplets enter the cells of the respiratory epithelium by docking their spike glycoproteins to the membrane-bound angiotensin converting enzyme 2 (ACE2)[1]. Subsequently, the infection can spread downwards the respiratory tree until it finally reaches the surfactant-producing alveolar type 2 pneumocytes. Successful infection of the lung cells leads to severe damage in gas exchange (O_2 uptake and CO_2 release), which provokes the dreadful symptomatology characterized by shortness of breath. The overall alveolar damage associated with progressive SARS-CoV-2 infection is difficult to treat and can lead to death[2,3]. Mechanisms of SARS-CoV-2 infection and tissue damage are studied in clinical patients[1], animal models[4] and in vitro models[5]. High-resolution imaging studies of alterations at the cellular level are critical to a complete understanding of the mechanisms of SARS-CoV-2 infection. We are presently exploiting the specific capabilities of scanning Helium-ion microscopy (HeIM) to study host-pathogen interactions in these three environments.

Helium-ion microscopy can image biological samples at nanometer resolution[6] after a minimal processing (often a formalin-fixation step) or even no processing (although SARS-CoV-2 infected samples require inactivation prior to imaging, for safety reasons). Due to its charge neutralization capability, HeIM can image biological samples (an insulating material) without the need of the electroconductive coating typically required by Scanning Electron Microscopy (SEM)[6]. This “no coating” capability of HeIM represents a great advantage as such coatings, even though only a few nanometers thick, can significantly alter and conceal fine details of biological structures.

Coronaviruses are enveloped viruses, surrounded by a host membrane acquired during the budding of virions through the host endoplasmic reticulum/Golgi apparatus. When the newly formed virions are released outside the cell, they propagate the infection using the ACE2 docking mechanism. Fresh bud

virions fuse their membrane with the one of the target cell and then release the viral genomic RNA inside the cytoplasm. The replication of new viruses “highjacks” several components of the intracellular vesicles machinery (newly replicated intracellular coronaviruses are found inside larger vesicular/vacuolar structures; they are not free as single virions inside the cytoplasm[7]). At this point, humoral and cellular immunity (antibodies and T-lymphocytes), and several other innate immune mechanisms (e.g., interferons and surfactant proteins), can interfere with this extra-cytoplasmic mechanism of infection. For example, the host immune system can neutralize the virus and eventually extinguish the infection. Indeed, several intervention strategies to control SARS-CoV-2 infection target the host immune defense to extra-cytoplasmic virions, like vaccination (which boosts the antibodies formation)[8]; convalescent plasma administration (which provides a high titer of neutralizing antibodies)[9]; laboratory-produced “cocktails” of neutralizing antibodies[10]. Unfortunately, several patients develop a hyper-acute inflammatory response, some of them on an autoimmune base[11], which can contribute to disease progression even in the absence of virions. This response can lead to a fatal multiorgan failure and subsequent death. Although therapeutic options are available, like corticosteroids[12] or cytokines adsorption[13], they cannot always control this often fatal progression of the coronavirus disease (COVID19). Despite a large percentage of the population in several countries being vaccinated, the occurrence of new symptomatic infections in individuals who were effectively vaccinated (“breakthrough infections” in vaccine-responders) has raised the question as to the cause of immune escape and renewed disease progression by SARS-CoV-2[14]. Vaccination significantly reduces the severity of infections, but a fraction of vaccinated individuals are re-infected with SARS-CoV-2 that can progress to an extremely severe illness and possible death[15]. Importantly, the viral entry mechanisms into the host cells are not fully understood and the question of how the virus transmits, infects and propagates in a host with robust immune response remains unanswered. In this study, we applied HeIM to interrogate the altered morphology of Vero E6 cells infected with mNeonGreen-expressing SARS-CoV-2. We demonstrate the presence of: 1)-long tunneling nanotubes (TNT) which strongly connect two or more cells over submillimeter distances; 2)-large scale multiple cell fusion events (syncytia); and 3)-abundant extracellular vesicles of various sizes, with unprecedented resolution. Based on the findings, we propose that these three ultrastructural features describe a fully intra-cytoplasmic connection among cells that may act as an alternative route of viral transmission and infection, disengaged from the conventional extra-cytoplasmic ACE2 docking mechanism. Futhermore, the intracytoplasmic viral transmission may explain the ability of SARS-CoV-2 to escape the immune surveillance and the host response.

2. Methods

2.1 Helium-ion microscopy

The principle of HeIM operation is very similar to SEM, except that the HeIM utilizes a beam of positively charged helium ions (He+) instead of negatively charged electrons to excite and detect secondary electrons from the sample surface[16]. Due to the high brightness and low energy spread of its atomically

sharp gas-field ion source, the smallest attainable focused spot size is about 0.3 nm. With its significantly smaller convergence angle compared to SEM, HeIM achieves a much larger depth of field[16], which is particularly useful for imaging three-dimensional structures. Due to their higher mass, He+ ions do not spread as much as electrons, resulting in a smaller escape volume of the secondary electrons and a higher surface resolution of the HeIM than SEM. A further benefit of HeIM is its charge compensation capability during secondary electron detection. In the HeIM, charges that accumulate on insulating samples are positive; so, a low-energy electron “flood gun”, which irradiates the sample with a diffuse beam of electrons, is used to achieve charge neutralization. This method eliminates the need for a conductive coating of samples and allows for direct visualization of their morphology at a nanoscale level[17]. A comprehensive review on the subject of bioimaging with HeIM has recently been published by Schmidt and co-workers[18].

We used a Zeiss Orion Plus helium ion microscope (Zeiss, Peabody MA, USA) at an acceleration voltage of 30 kV and chamber base pressure of $3x10^{-7}$ Torr. The typical Helium beam had a 0.7 pA current which was achieved by varying the spot control between 5 and 6 to adjust lens 1, coupled with using 10 µm aperture. The sample stage was tilted by 10°, and the working distance was kept in the 8-10mm range. Since all the studied samples were nonconductive, the electron flood gun was used to eliminate charging effects, with an electron flood time of 10 µs and He^+ beam dwell time of 0.2µs.

2.2 Vero E6 cell culture and SARS-CoV-2 infection

The African green monkey kidney epithelial cell line (Vero E6) has been used extensively for SARS-CoV research in cell culture-based infection models. The lineage was developed in 1962 by Yasumura and Kawakita at the Chiba University in Japan deriving cells from a female of Chlorocebus sabaeus[5]. Vero E6 cells support SARS-CoV-2 replication in culture, while many more cell lines have been reported to be refractory to SARS-CoV-2 infection[19]. The close phylogenetic relationship between SARS-CoV and SARS-CoV-2, the abundantly expressed ACE2 on the Vero E6 membrane, and their characteristic of being deficient in interferon-alpha or beta[20], could explain their susceptibility to SARS-CoV-2 infection.

All the work involving infectious SARS-CoV-2 was performed in the biosafety level 3 facilities at Rutgers University. The SARS-CoV-2 expressing mNeonGreen was provided by Dr. Theresa Chang (Rutgers University) and Dr. Pei-Yong Shi (University of Texas)[21]. Vero E6 cells were grown in Dulbecco’s modified essential medium (DMEM) (Ca# D6429, Sigma-Aldrich, USA) containing 10% fetal bovine sera (FBS) (Sigma-Aldrich, USA). For SARS-CoV-2 infection, $0.3x10^6$ Vero E6 cells were seeded onto a 13mm diameter glass coverslips with carved reference frames, in a six-well cell-culture plate with 2mL of DMEM+FBS media. At 18-24 hours post-seeding, the spent media was aspirated. The cells were infected with SARS-CoV-2 expressing mNeonGreen at a multiplicity of infection (MOI) of 0.1 (i.e., 1 viral particle for 10 host cells) in 400 µL of FBS-free DMEM. The plates were incubated at 37˚C for 1 hour with intermittent rocking for infection. Then the wells were replenished with 2 mL of DMEM + FBS. At 24 hours post-infection, the cell culture supernatants were removed and the cells were fixed with 4% paraformaldehyde (Cat# 19943-k2, Thermo Scientific, USA) as described previously[22].

2.3 Correlative microscopy

Reference frames carved on the glass coverslips allowed us to perform correlative HeIM-Fluorescence-Phase Contrast microscopy (Zeiss Axio Observer, Zeiss Jena D). The ability to practically identify and study the same cell in these three different imaging modalities was extremely useful, as we could merge information specifically provided by each of them. As HeIM does not require any electroconductive coating, samples imaged by HeIM could be re-imaged with phase contrast or fluorescence microscopy, as needed. Samples imaged in phase contrast and fluorescence microscopy were in the hydrated state in the culture well. They were dehydrated and put under high vacuum at $3x10^{-7}$ Torr for HeIM imaging, but they were eventually re-hydrated without any damage to the cellular structures if a new phase-contrast and/or fluorescence microscopy imaging was required. Vero E6 cells infected with SARS-CoV-2 were identified by the green fluorescence of the mNeonGreen protein expressed by the virus intracellularly. We were able to detect the green fluorescence with a filter set at excitation peak at 488 nm and an emission peak at 509 nm, with a Zeiss Axiocam 305 CCD camera and Zeiss Zen Blue 2.6 software (the optimal excitation and emission peaks for mNeonGreen protein are at 506 nm and 517 nm, respectively[23]).

3. Results

3.1 Inter-cellular connections by Tunneling Nano Tubes

It has been reported that SARS-CoV-2 infected Vero E6 cells produce many filopodia, and they are longer than those present in uninfected cells[24,25]. We observed these very long filopodia and followed their path. We confirmed that such long filopodia are not present in uninfected cells (Figure 1). These filopodia are visualized even at nanometer diameters using HeIM, providing high-resolution imaging of their surface details. It would be difficult to observe these finer details with conventional optical microscopy. Based on our observations, these very long filopodia showed the characteristics of Tunneling Nano Tubes (TNT) (see Discussion for the terms “cytonemes” and “TNT” and how they differ from filopodia). These TNT connect two or more infected host cells over submillimeter distances (Figure 2). They often exceed 40 microns in length and span distances which encompass several cells (Figure 3). They generally start with a “growth cone” of specific morphology (Figure 4); a smaller diameter tube is sometimes observed stemming from it (Figure 5). Some infected cells bulge and detach from the floor, while emitting TNT in a specific asymmetric bipolar fashion (Figure 5). These TNT keep their individual structure when they cross other TNT, but they may fuse their membrane when overlapping with another cell (Figure 6). Structures resembling vesicles or mitochondria have been imaged at this fusion point of entry/exit with the cell (Figure 3). Some TNTs appear under mechanical tension between two cells. In these cases, we documented TNT pulling on both cells resulting in a stretched morphology. We ruled out the possibility that this tension could be caused by the dehydration process because correlative microscopy showed the same stretched morphology in the hydration state in phase-contrast microscopy prior to HeIM. Stretched TNT between two cells often presents a bulging mid-way (Figure 7). However, the dehydration process likely caused breakages at the TNT origin close to the cell body; when this occurred, we visualized an

inner content of cylindrical structures of about 25 nm in diameter (Figure 4), suggestive of microtubules. TNT in their larger diameter showed similar longitudinal cytoskeletal features underlining the membrane, and they showed regions of bulging content (Figure 3): this feature is reminiscent of pictures of axonal transport. There were also clear images of spherical bulging along the length of TNT (Figure 3). Notably, we could visualize regions of 250 nm^2 or larger, where several cells showed to be connected either by TNT or by fusion (membrane continuity) and, at the same time, extracellular vesicles were present all around, meaning that these three features co-exist together in the same cell (Figure 2).

3.2 Cell fusion

The virus propagating within Vero E6 cells causes severe cytopathic effect (CPE)[5]. It is possible that the uninfected cells that should lie flat over the well-floor, can swell and detach from the floor, may fuse together and may form TNT. However, we identified that SARS-CoV-2 infected Vero E6 cells can form large-scale (submillimeter) clusters of multiple fused cells (syncytia) at 24 hours post-infection. This type of fusion is not observed in uninfected cells. HelM provided images of the homogeneous continuity of the membrane of the syncytia (Figure 8, A and B). Correlative microscopy showed the presence of multiple DAPI stained fluorescent nuclei in clusters of cells (Figure 8).

3.3 Extracellular vesicles

Many spherical vesicles whose diameter ranged from about 30 nm to more than 1 micron have been observed both in SARS-CoV-2 infected and uninfected Vero E6 cells, apparently in similar numbers (Figure 1 and 9). We documented the extracellular vesicles when they bud from the cell membrane (Figure 1A3, 1B3, 9B), or while they are in contact with the membrane (Figure 9A and C), or as free objects in the extracellular space (figure1C). Apoptotic bodies were observed budding from infected cells (Figure 9D); some of them were captured just before leaving a disintegrating cell (Figure 10B). A finding that can be put in relation to the presence of extracellular vesicles is that both infected and uninfected VeroE6 cells showed a significant presence of caveolae (Figure 1 and Figure 9E and F). These “holes” in the cell membrane have been previously observed in not-electroconductive-coated mammalian cells; they are the circular aperture of larger spherical cavities formed by the scaffolding “caveolins” proteins[26]. Prior studies using HelM have reported the caveolae as lipid nanodomains[17]. Importantly, caveolae can be both entry or exit points for vesicles in the diameter range of the SARS-CoV-2[27,28].

4. Discussion

TNT-mediated inter-cellular connections. TNTs are tubular structures of nanometer-to-micrometer diameters that connect the cytoplasm of adjacent or distant cells, thus providing an intracytoplasmic passage to exchange and/or transport biomolecules as small as ions, lipids, nucleic acids, microRNA, cytoplasmic proteins, or as big as whole organelles, such as endosomes, lysosomes, mitochondria and portions of the endoplasmic reticulum or Golgi apparatus. They can be very long, notably over

submillimeter distances (spanning several cell diameters)[29–36]. TNTs are reported to be transient structures and can form or disintegrate in a matter of a minutes[29]. They are documented to promote the spread of various pathogens, including viruses[37,38], prions[39], fungi[40] and mycoplasma[41].

TNT were initially hypothesized as a subset of filopodia, but accumulating evidence suggests that TNT are categorically different from filopodia, both in length (longer than filopodia), diameter (as thin as filopodia but as large as axons), composition and function. Unlike TNT, filopodia are not capable of mediating vesicular transport. Filopodia are made of F-actin, while TNT, despite being composed of F-actin in their vast majority, can incorporate microtubules too, or be mainly composed of microtubules[42]. Some authors have named long-filopodial bridges containing F-actin as “cytonemes” and differentiated them from TNT[43–45]. We recognize that TNT is now the most accepted term in the literature, even if there are structural variations among them that may justify a further sub-classification. With their growth cone, length, potential microtubule skeleton, and intraluminal transport, TNT resemble the neuronal axons[46]. TNTs may form gap-like junctions between two connected cells over a short distance and extend when the two connected cells migrate apart. We documented this mechanical stretch, the capability of TNT to withstand it, and the presence of bulging(s) mid-way. While it is possible that this bulging represents a fusion of two growth cones originating from different cells, or some other phenomenon associated with intraluminal cargo transport, it is also likely that the bulging is just a physical response to the stretching and thinning of the nanotube[47]. TNT may keep its structure when overlapping cells are present in between the two distant cells that they connect. However, we documented the occurrence of possible membrane fusion of overlapping TNT with cells in between, thus suggesting the possibility that the cytoplasm of multiple cells may be connected through a single TNT. Like in axonal transport, TNT diameter enlarges when a bulky content is transported inside. The spherical morphology of some of these contents has been clearly captured by HeIM, which suggests that the transport of vesicles or viral particles is possible through TNTs.

The role of TNTs in SARS-COV-2 infection has been discussed in two recent papers[32,33]. TNT-mediated intracellular spread can protect the viruses from the circulating immune surveillance and possible viral-neutralization activity present in the extracellular matrix. Intercellular viral spread via TNT avoids virus-cell interactions that may initiate host defense signaling and mount antiviral responses. Many viruses, such as the influenza virus, human immunodeficiency virus (HIV), and herpes simplex virus (HSV), can evade host immunity and avoid pharmaceutical targeting by using TNT to transmit their genomes to naïve/new cells. Our observations using HeIM images make it reasonable to add SARS-CoV-2 to the list of viruses that can transmit and cause infection between host cells through TNT. Consistent with this notion, we did not observe any TNT formation in the uninfected Vero E6 cells.

Cell fusion. Cell-cell fusion (a.k.a. Syncytia) can be induced by certain types of viral infections, such as HIV, respiratory syncytial virus, and HSV[48]. Syncytia formation has been reported in the literature associated with SARS-COV-2 infection[49–51], most notably in histopathologic lung sections from patients who died from COVID-19[51]. Another relevant finding is that Vero E6 cells, upon expressing the SARS-CoV-

2 spike protein, could form syncytia as long as the ACE2 is present, but they cannot when transfected with SARS- CoV spike protein[50], implying that cell fusion capability may be specific to SARS-CoV-2. It is reasonable to think that virus-induced cell fusion can facilitate the transfer of the viral genome to the neighboring cells[49] by sharing cytoplasm between the cells. We observed significant Syncytia events only in the SARS-CoV-2 infected Vero E6 cells and not in the uninfected cells.

Extracellular vesicles. Cell-cell communication can be mediated by factors released in the intercellular space, such as hormones, cytokines, and other inflammatory mediators. The general term extracellular vesicles (EV) refers to any membrane vesicle released into the extracellular space. An accepted classification defines vesicles generated inside the cell and released into the extracellular space as “exosomes,” (diameter range from 30 to 150 nm). In contrast, vesicles pinched off from the plasma membrane are called “microvesicles” (diameter range from 150 to 1000 nm)[52,53]. Some Authors consider apoptotic bodies (bulk protrusions from dying cells that may end up in extracellular vesicles of 800nm diameter or larger) as part of the EV family. For a long time, EV were considered as “cellular dust” and did not attract much attention from researchers[53]. However, EV have recently been found to play key roles in cell-cell communication, allowing cells to exchange proteins, lipids and genetic material[27,54].

Viruses might use EV to infect naïve/new cells[55]. The physical and chemical characteristics of many EV, as well as their biogenesis pathways, resemble those of retroviruses. EV generated by virus-infected cells can incorporate viral proteins and fragments of viral RNA, which is similar to the defective (noninfectious) retroviruses. EV are known to facilitate HIV-1 infection and dissemination; HIV-1 has been reported as “entrapped” in exosome aggregates[56]. “Trojan” exosomes might provide retroviruses the ability to take advantage of the cell-encoded intercellular vesicle traffic[56–58]. HIV-1 exploits the surface properties of the exosomes to facilitate rapid infection of progeny virus, and in so doing, camouflages the virus from immune surveillance. Surrounding itself with exosomes, HIV-1 can accelerate its infection and dissemination[56]. It has been hypothesized that SARS-CoV-2 infected cells can release EV with viral antigens or cargo. EV acting as a “Trojan horse” could explain the re-appearance of the viral RNA in patients recovered from COVID-19 [28,59]. EV are involved in SARS-CoV-2 infection[60–62] and could be used as biomarkers of disease severity[63]. SARS-CoV-2 RNA has been identified in the exosomal cargo of samples from patients with COVID-19, but not in healthy subjects, suggesting that the virus might use the endocytosis route to spread infection[64].

Extracellular vesicles can convey pathogen molecules that serve as antigens or agonists of innate immune receptors to induce host defense and immunity or serve as regulators of host defense and mediators of immune evasion[54,56]. We speculate that the mechanism of camouflaging the virus from immune surveillance might rather trigger an autoimmune response from the host in those instances where the close association of viral and host antigens promotes their crossed-recognition.

The intra-cytoplasmic route of SARS-COV-2 transmission. The nanometer resolution, lack of coating and practical imaging of samples provided by scanning HelM suggest that SARS-CoV-2 infected Vero E6 cells

can establish connections by TNT. HeIM also confirmed that they could form syncytia and exchange EV. These three features co-exist together in space and time. In all three processes, there is an exchange of cytoplasmic content between host cells. This may likely be an alternative route of transmission and infection, clearly distinct from the well-known, conventional extra-cytoplasmic ACE2 (or other receptor-mediated) docking mechanism. Even if the close phylogenetic relationship between SARS-CoV and SARS-CoV-2 makes it reasonable to translate much of our knowledge of SARS-CoV to SARS-CoV-2, we should focus on the differences between SARS-CoV and SARS-CoV-2 to explain divergent clinical patterns of disease caused by these two viruses. We already cited the fusogenic potential specific to the SARS-CoV-2 spike protein, but not the SARS-CoV spike protein[50]. Notably, SARS-CoV-2 has a lower density of spikes and can produce a high number of defective copies (with little or no spikes) released outside the infected cell[65,66]. These observations seem like strong, even if indirect, evidence that an alternative route of viral propagation must be in place for SARS-CoV-2.

The intra-cytoplasmic route can hide the virus from the host immune surveillance and potential anti viral response, based on the detection of the extracellular virions. In the intra-cytoplasmic route, naïve cells could be infected by viral mRNA, transmitted free, or in the form of cargo in micro-vesicles. Defective virions, presenting little or no spikes, which would be defective to infect other cells via the extra-cytoplasmic route, might become infective when transmitted via the intra-cytoplasmic route. Host defenses based on a humoral or cellular immune response are mostly ineffective against this intra-cytoplasmic spreading of SARS-CoV-2. More than two decades of failure to realize a protective vaccine for HIV highlights the need for a better understanding of the viral immune evasion mechanisms[56], and we wonder if a similar case is mounting for SARS-CoV-2.

Clinical relevance. The vast majority of diseases, including COVID-19, are complex in their disease presentation and have multiple stages, and each stage may have a specific/targeted and generic/multiple targets therapeutic approach (many forms of cancer fit in this description). Specific drugs that interfere with the intra-cytoplasmic route of viral transmission described in this report can be promising therapeutic candidates to treat COVID19. Analyzing the spectrum of possible therapeutic molecules that impair the intracytoplasmic route of viral transmission is beyond the scope of this paper. However, we report that some suitable drugs have been tested already. In targeting TNT, the proven clinical efficacy in treating COVID19 of Colchicine, a microtubule inhibitor that might interfere with TNT formation[67,68], can be suggestive evidence of the role of TNT in COVID19 pathogenesis. Drugs that suppress cell fusion have been tested in vitro[51]; among them, niclosamide, an oral anti-helminthic agent, was effective in cell protection against virus-induced cell death[49,51]. Drugs that interfere with EV machinery at large have been tested even before the COVID-19 pandemic. Chloroquine is well-known for elevating endosomal pH and has been shown to be effective against SARS-CoV infection in vitro[69] and in COVID-19 cases[70]. In their interference with the cytoplasmic route, these drugs likely need to be administered during the early stages of SARS-CoV-2 infection and should be considered to have a limited or no preventive capability.

Limitations in our study include the absence of wider use of specific markers to track the viral transmission and usage of primary human cells to confirm our findings. However, observations reported here are actually stimuli for planning new studies not only by us but also by the larger scientific community. Having highlighted the presence of a potential intracytoplasmic route for SARS-COV-2 transmission and infection can provide a pathophysiological explanation for how therapies already in use may work and promote efforts towards the identification of new therapeutic agents.

Declarations

Acknowledgements

Authors would like to acknowledge Robert Bartynski, Hussein Hijazi (RU Physics & Astronomy); David Alland, Theresa Chang (RU PHRI); Pei-Yong Shi (University of Texas); Jason Kaelber (RU IQB); Vincent Cancellieri, Russ Mello, Shawn McVey, John Notte (Zeiss, Peabody MA); Gary Brewer; Mei Ling Li (RU RBHI) for their contribution to different stages of this effort that started in March 2020. This study was partially funded by the National Science Foundation grant NSF 2115363 “RAPID /SARS-CoV-2 host cell interactions: quantitative investigations via Scanning Helium-ion Microscopy”, awarded to LF and AM. S.S. received financial support from the Rutgers Center for COVID-19 Research and Pandemic Preparedness (CCRP2; Project# 302211).

Author contributions:

Antonio Merolli: design of the study; optical imaging; HeIM imaging; principal writer of the manuscript.

Leila Kasaei: HeIM imaging; review of the manuscript.

Santhamani Ramsamy: virus and host cell cultures; optical imaging.

Afsal Kolloli: virus and host cell culture.

Ranjeet Kumar: virus and host cell culture.

Selvakumar Subbian: design of the study; supervision of SARS-CoV-2 studies; writing of the manuscript.

Leonard Feldman: design of the study; HeIM imaging; writing of the manuscript.

Competing interests: none

Materials & Correspondence: Antonio Merolli is the author to whom correspondence and material requests should be addressed.

Related manuscripts: there are no related manuscripts with overlapping authorship that are under consideration or in press at other journals

References

1. Zhao, C. L. *et al.* Pathological findings in the postmortem liver of patients with coronavirus disease 2019 (COVID-19). *Hum Pathol* **109**, 59–68, doi:10.1016/j.humpath.2020.11.015 (2021).
2. Martines, R. B. *et al.* Pathology and Pathogenesis of SARS-CoV-2 Associated with Fatal Coronavirus Disease, United States. *Emerg Infect Dis* **26**, 2005–2015, doi:10.3201/eid2609.202095 (2020).
3. Deshmukh, V., Motwani, R., Kumar, A., Kumari, C. & Raza, K. Histopathological observations in COVID-19: a systematic review. *J Clin Pathol* **74**, 76–83, doi:10.1136/jclinpath-2020-206995 (2021).
4. Braxton, A. M. *et al.* Hamsters as a Model of Severe Acute Respiratory Syndrome Coronavirus-2. *Comp Med*, doi:10.30802/aalas-cm-21-000036 (2021).
5. Ogando, N. S. *et al.* SARS-coronavirus-2 replication in Vero E6 cells: replication kinetics, rapid adaptation and cytopathology. *J Gen Virol* **101**, 925–940, doi:10.1099/jgv.0.001453 (2020).
6. Joens, M. S. *et al.* Helium Ion Microscopy (HIM) for the imaging of biological samples at sub-nanometer resolution. *Sci Rep* **3**, 3514, doi:10.1038/srep03514 (2013).
7. Bullock, H. A., Goldsmith, C. S. & Miller, S. E. Best practices for correctly identifying coronavirus by transmission electron microscopy. *Kidney Int* **99**, 824–827, doi:10.1016/j.kint.2021.01.004 (2021).
8. Fan, Y. J., Chan, K. H. & Hung, I. F. Safety and Efficacy of COVID-19 Vaccines: A Systematic Review and Meta-Analysis of Different Vaccines at Phase 3. *Vaccines (Basel)* **9**, doi:10.3390/vaccines9090989 (2021).
9. Roback, J. D. & Guarner, J. Convalescent Plasma to Treat COVID-19: Possibilities and Challenges. *Jama* **323**, 1561–1562, doi:10.1001/jama.2020.4940 (2020).
10. Weinreich, D. M. *et al.* REGN-COV2, a Neutralizing Antibody Cocktail, in Outpatients with Covid-19. *N Engl J Med* **384**, 238–251, doi:10.1056/NEJMoa2035002 (2021).
11. McMillan, P., Dexhiemer, T., Neubig, R. R. & Uhal, B. D. COVID-19-A Theory of Autoimmunity Against ACE-2 Explained. *Front Immunol* **12**, 582166, doi:10.3389/fimmu.2021.582166 (2021).
12. Kim, W. Y., Kweon, O. J., Cha, M. J., Baek, M. S. & Choi, S. H. Dexamethasone may improve severe COVID-19 via ameliorating endothelial injury and inflammation: A preliminary pilot study. *PLoS One* **16**, e0254167, doi:10.1371/journal.pone.0254167 (2021).

13. Ruiz-Rodríguez, J. C., Molnar, Z., Deliargyris, E. N. & Ferrer, R. The Use of CytoSorb Therapy in Critically Ill COVID-19 Patients: Review of the Rationale and Current Clinical Experiences. *Crit Care Res Pract* 2021, 7769516, doi:10.1155/2021/7769516 (2021).
14. Bergwerk, M. *et al.* Covid-19 Breakthrough Infections in Vaccinated Health Care Workers. *N Engl J Med*, doi:10.1056/NEJMoa2109072 (2021).
15. Bahl, A. *et al.* Vaccination reduces need for emergency care in breakthrough COVID-19 infections: A multicenter cohort study. *Lancet Reg Health Am*, 100065, doi:10.1016/j.lana.2021.100065 (2021).
16. Wirtz, T., De Castro, O., Audinot, J. N. & Philipp, P. Imaging and Analytics on the Helium Ion Microscope. *Annu Rev Anal Chem (Palo Alto Calif)* **12**, 523–543, doi:10.1146/annurev-anchem-061318-115457 (2019).
17. Schürmann, M. *et al.* Helium Ion Microscopy Visualizes Lipid Nanodomains in Mammalian Cells. *Small* **11**, 5781–5789, doi:10.1002/smll.201501540 (2015).
18. Schmidt, M., Byrne, J. M. & Maasilta, I. J. Bio-imaging with the helium-ion microscope: A review. *Beilstein J Nanotechnol* **12**, 1–23, doi:10.3762/bjnano.12.1 (2021).
19. Takayama, K. In Vitro and Animal Models for SARS-CoV-2 research. *Trends Pharmacol Sci* **41**, 513–517, doi:10.1016/j.tips.2020.05.005 (2020).
20. Desmyter, J., Melnick, J. L. & Rawls, W. E. Defectiveness of interferon production and of rubella virus interference in a line of African green monkey kidney cells (Vero). *J Virol* **2**, 955–961, doi:10.1128/jvi.2.10.955-961.1968 (1968).
21. Xie, X. *et al.* An Infectious cDNA Clone of SARS-CoV-2. *Cell Host Microbe* **27**, 841-848.e843
, doi:10.1016/j.chom.2020.04.004 (2020).
22. Kumar, R., Kolloli, A. & Subbian, S. Inactivation and Elimination of SARS-CoV-2 in Biosamples Using Simple Fixatives and Ultrafiltration. *Methods Protoc* **4**, doi:10.3390/mps4010018 (2021).
23. Shaner, N. C. *et al.* A bright monomeric green fluorescent protein derived from Branchiostoma lanceolatum. *Nat Methods* **10**, 407–409, doi:10.1038/nmeth.2413 (2013).
24. Bouhaddou, M. *et al.* The Global Phosphorylation Landscape of SARS-CoV-2 Infection. *Cell* **182**, 685–712
.e619
, doi:10.1016/j.cell.2020.06.034 (2020).
25. Barreto-Vieira, D. F. *et al.* Morphology and morphogenesis of SARS-CoV-2 in Vero-E6 cells. *Mem Inst Oswaldo Cruz* **116**, e200443, doi:10.1590/0074-02760200443 (2021).
26. Nassoy, P. & Lamaze, C. Stressing caveolae new role in cell mechanics. *Trends Cell Biol* **22**, 381–389, doi:10.1016/j.tcb.2012.04.007 (2012).
27. van Niel, G., D'Angelo, G. & Raposo, G. Shedding light on the cell biology of extracellular vesicles. *Nat Rev Mol Cell Biol* **19**, 213–228, doi:10.1038/nrm.2017.125 (2018).

28. Chatterjee, V., Yang, X., Ma, Y., Wu, M. H. & Yuan, S. Y. Extracellular vesicles: new players in regulating vascular barrier function. *Am J Physiol Heart Circ Physiol* **319**, H1181-h1196, doi:10.1152/ajpheart.00579.2020 (2020).
29. Gurke, S., Barroso, J. F. & Gerdes, H. H. The art of cellular communication: tunneling nanotubes bridge the divide. *Histochem Cell Biol* **129**, 539–550, doi:10.1007/s00418-008-0412-0 (2008).
30. Kimura, S., Hase, K. & Ohno, H. Tunneling nanotubes: emerging view of their molecular components and formation mechanisms. *Exp Cell Res* **318**, 1699–1706, doi:10.1016/j.yexcr.2012.05.013 (2012).
31. Karlikow, M. *et al.* Drosophila cells use nanotube-like structures to transfer dsRNA and RNAi machinery between cells. *Sci Rep* **6**, 27085, doi:10.1038/srep27085 (2016).
32. Zhang, S., Kazanietz, M. G. & Cooke, M. Rho GTPases and the emerging role of tunneling nanotubes in physiology and disease. *Am J Physiol Cell Physiol* **319**, C877-c884, doi:10.1152/ajpcell.00351.2020 (2020).
33. Tiwari, V., Koganti, R., Russell, G., Sharma, A. & Shukla, D. Role of Tunneling Nanotubes in Viral Infection, Neurodegenerative Disease, and Cancer. *Front Immunol* **12**, 680891, doi:10.3389/fimmu.2021.680891 (2021).
34. Zhu, H. *et al.* Rab8a/Rab11a regulate intercellular communications between neural cells via tunneling nanotubes. *Cell Death Dis* **7**, e2523, doi:10.1038/cddis.2016.441 (2016).
35. Rustom, A., Saffrich, R., Markovic, I., Walther, P. & Gerdes, H. H. Nanotubular highways for intercellular organelle transport. *Science* **303**, 1007–1010, doi:10.1126/science.1093133 (2004).
36. Osswald, M. *et al.* Brain tumour cells interconnect to a functional and resistant network. *Nature* **528**, 93–98, doi:10.1038/nature16071 (2015).
37. Eugenin, E. A., Gaskill, P. J. & Berman, J. W. Tunneling nanotubes (TNT) are induced by HIV-infection of macrophages: a potential mechanism for intercellular HIV trafficking. *Cell Immunol* **254**, 142–148, doi:10.1016/j.cellimm.2008.08.005 (2009).
38. Kumar, A. *et al.* Influenza virus exploits tunneling nanotubes for cell-to-cell spread. *Sci Rep* **7**, 40360, doi:10.1038/srep40360 (2017).
39. Gousset, K. & Zurzolo, C. Tunnelling nanotubes: a highway for prion spreading? *Prion* **3**, 94–98, doi:10.4161/pri.3.2.8917 (2009).
40. Bloemendal, S. & Kück, U. Cell-to-cell communication in plants, animals, and fungi: a comparative review. *Naturwissenschaften* **100**, 3–19, doi:10.1007/s00114-012-0988-z (2013).
41. Kim, B. W., Lee, J. S. & Ko, Y. G. Mycoplasma exploits mammalian tunneling nanotubes for cell-to-cell dissemination. *BMB Rep* **52**, 490–495, doi:10.5483/BMBRep.2019.52.8.243 (2019).
42. Vignais, M. L., Caicedo, A., Brondello, J. M. & Jorgensen, C. Cell Connections by Tunneling Nanotubes: Effects of Mitochondrial Trafficking on Target Cell Metabolism, Homeostasis, and Response to Therapy. *Stem Cells Int* 2017, 6917941, doi:10.1155/2017/6917941 (2017).
43. Sherer, N. M. & Mothes, W. Cytonemes and tunneling nanotubules in cell-cell communication and viral pathogenesis. *Trends Cell Biol* **18**, 414–420, doi:10.1016/j.tcb.2008.07.003 (2008).

44. Abounit, S. & Zurzolo, C. Wiring through tunneling nanotubes–from electrical signals to organelle transfer. *J Cell Sci* **125**, 1089–1098, doi:10.1242/jcs.083279 (2012).
45. Ramírez-Weber, F. A. & Kornberg, T. B. Cytonemes: cellular processes that project to the principal signaling center in Drosophila imaginal discs. *Cell* **97**, 599–607, doi:10.1016/s0092-8674(00)80771-0 (1999).
46. Nussenzveig, H. M. Are cell membrane nanotubes the ancestors of the nervous system? *Eur Biophys J* **48**, 593–598, doi:10.1007/s00249-019-01388-x (2019).
47. Martínez-Calvo, A., Rivero-Rodríguez, J., Scheid, B. & Sevilla, A. Natural break-up and satellite formation regimes of surfactant-laden liquid threads. *Journal of Fluid Mechanics* **883**, A35, doi:10.1017/jfm.2019.874 (2020).
48. Leroy, H. *et al.* Virus-Mediated Cell-Cell Fusion. *Int J Mol Sci* **21**, doi:10.3390/ijms21249644 (2020).
49. Lin, L., Li, Q., Wang, Y. & Shi, Y. Syncytia formation during SARS-CoV-2 lung infection: a disastrous unity to eliminate lymphocytes. *Cell Death Differ* **28**, 2019–2021, doi:10.1038/s41418-021-00795-y (2021).
50. Zhang, Z. *et al.* SARS-CoV-2 spike protein dictates syncytium-mediated lymphocyte elimination. *Cell Death Differ* **28**, 2765–2777, doi:10.1038/s41418-021-00782-3 (2021).
51. Braga, L. *et al.* Drugs that inhibit TMEM16 proteins block SARS-CoV-2 spike-induced syncytia. *Nature* **594**, 88–93, doi:10.1038/s41586-021-03491-6 (2021).
52. Colombo, M., Raposo, G. & Théry, C. Biogenesis, secretion, and intercellular interactions of exosomes and other extracellular vesicles. *Annu Rev Cell Dev Biol* **30**, 255–289, doi:10.1146/annurev-cellbio-101512-122326 (2014).
53. Nolte-'t Hoen, E., Cremer, T., Gallo, R. C. & Margolis, L. B. Extracellular vesicles and viruses: Are they close relatives? *Proc Natl Acad Sci U S A* **113**, 9155–9161, doi:10.1073/pnas.1605146113 (2016).
54. Schorey, J. S. & Harding, C. V. Extracellular vesicles and infectious diseases: new complexity to an old story. *J Clin Invest* **126**, 1181–1189, doi:10.1172/jci81132 (2016).
55. Urbanelli, L. *et al.* The Role of Extracellular Vesicles in Viral Infection and Transmission. *Vaccines (Basel)* **7**, doi:10.3390/vaccines7030102 (2019).
56. Kadiu, I., Narayanasamy, P., Dash, P. K., Zhang, W. & Gendelman, H. E. Biochemical and biologic characterization of exosomes and microvesicles as facilitators of HIV-1 infection in macrophages. *J Immunol* **189**, 744–754, doi:10.4049/jimmunol.1102244 (2012).
57. Gould, S. J., Booth, A. M. & Hildreth, J. E. The Trojan exosome hypothesis. *Proc Natl Acad Sci U S A* **100**, 10592–10597, doi:10.1073/pnas.1831413100 (2003).
58. Hildreth, J. E. K. HIV As Trojan Exosome: Immunological Paradox Explained? *Front Immunol* **8**, 1715, doi:10.3389/fimmu.2017.01715 (2017).
59. Elrashdy, F., Aljaddawi, A. A., Redwan, E. M. & Uversky, V. N. On the potential role of exosomes in the COVID-19 reinfection/reactivation opportunity. *J Biomol Struct Dyn*, 1–12, doi:10.1080/07391102.2020.1790426 (2020).

60. Rosell, A. *et al.* Patients With COVID-19 Have Elevated Levels of Circulating Extracellular Vesicle Tissue Factor Activity That Is Associated With Severity and Mortality. *Arterioscler Thromb Vasc Biol* **41**, Atvbaha120315547, doi:10.1161/atvbaha.120.315547 (2020).
61. Guervilly, C. *et al.* Dissemination of extreme levels of extracellular vesicles: tissue factor activity in patients with severe COVID-19. *Blood Adv* **5**, 628–634, doi:10.1182/bloodadvances.2020003308 (2021).
62. Sur, S. *et al.* Exosomes from COVID-19 Patients Carry Tenascin-C and Fibrinogen-β in Triggering Inflammatory Signals in Cells of Distant Organ. *Int J Mol Sci* **22**, doi:10.3390/ijms22063184 (2021).
63. Cappellano, G. *et al.* Circulating Platelet-Derived Extracellular Vesicles Are a Hallmark of Sars-Cov-2 Infection. *Cells* **10**, doi:10.3390/cells10010085 (2021).
64. Barberis, E. *et al.* Circulating Exosomes Are Strongly Involved in SARS-CoV-2 Infection. *Front Mol Biosci* **8**, 632290, doi:10.3389/fmolb.2021.632290 (2021).
65. Ke, Z. *et al.* Structures and distributions of SARS-CoV-2 spike proteins on intact virions. *Nature* **588**, 498–502, doi:10.1038/s41586-020-2665-2 (2020).
66. Laue, M. *et al.* Morphometry of SARS-CoV and SARS-CoV-2 particles in ultrathin plastic sections of infected Vero cell cultures. *Sci Rep* **11**, 3515, doi:10.1038/s41598-021-82852-7 (2021).
67. Knack, R. S., Losso, L. C., Knack, R. S. & Hanada, T. Preliminary results of clinical use of colchicine in COVID-19 treatment. *BMJ Case Rep* **14**, doi:10.1136/bcr-2021-244482 (2021).
68. Lien, C. H. *et al.* Repurposing Colchicine in Treating Patients with COVID-19: A Systematic Review and Meta-Analysis. *Life (Basel)* **11**, doi:10.3390/life11080864 (2021).
69. Vincent, M. J. *et al.* Chloroquine is a potent inhibitor of SARS coronavirus infection and spread. *Virol J* **2**, 69, doi:10.1186/1743-422x-2-69 (2005).
70. Derwand, R. & Scholz, M. Does zinc supplementation enhance the clinical efficacy of chloroquine/hydroxychloroquine to win today's battle against COVID-19? *Med Hypotheses* **142**, 109815, doi:10.1016/j.mehy.2020.109815 (2020).

Figures

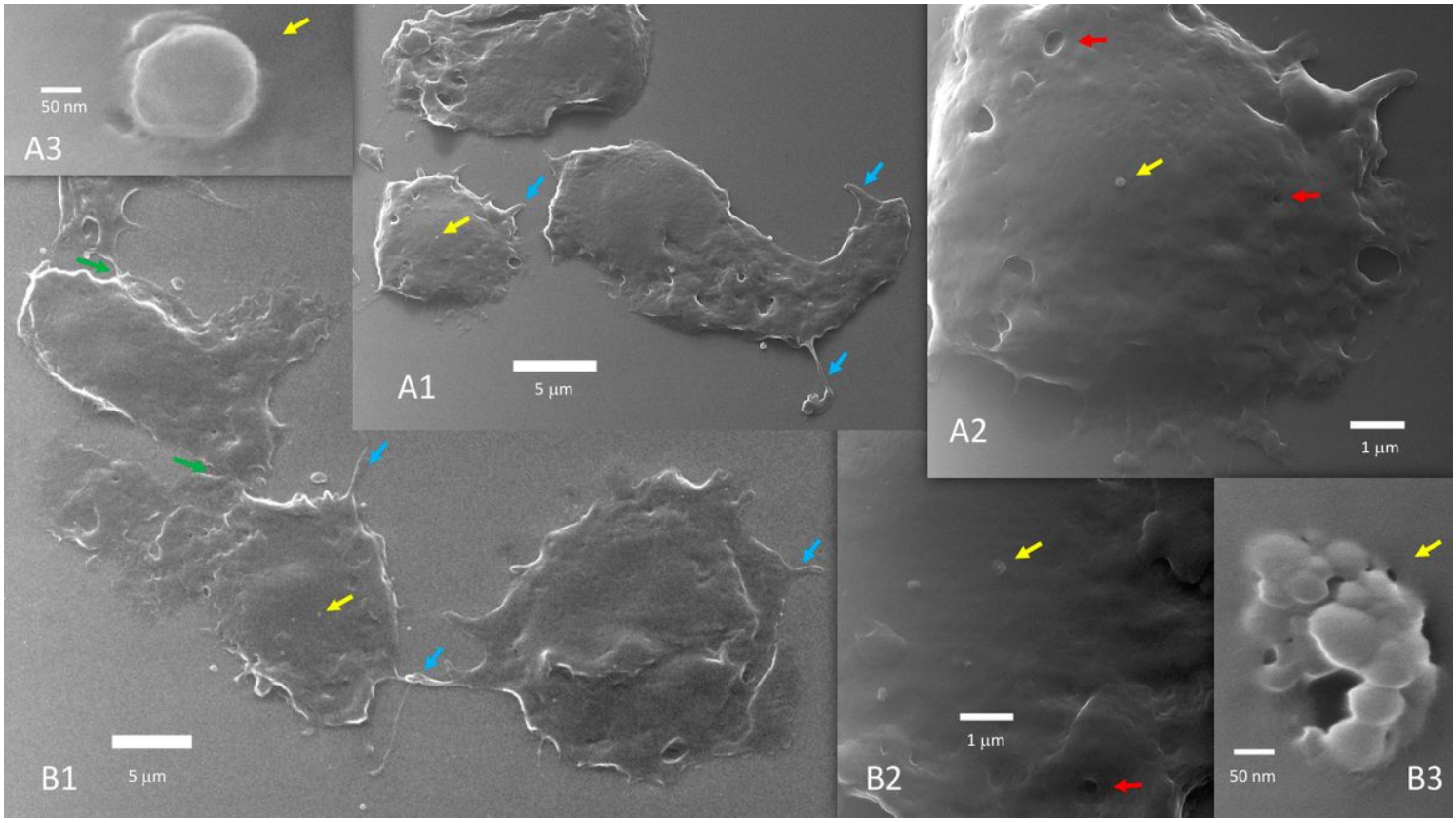

Figure 1

Uninfected Vero E6 cells. Uninfected cells do not fuse during growth and when progressing toward confluency. Coarse filopodia (blue arrows) and caveolae (red arrows) are present in these cells. There are bridge points of contact (green arrows). Vesicles can be seen over the cell surface (yellow arrows) or close to the cells. In A3, a 200 nm vesicle is seen budding or merging at the cell membrane level. B3 likely captured the exosomes discharge from a multivesicular body.

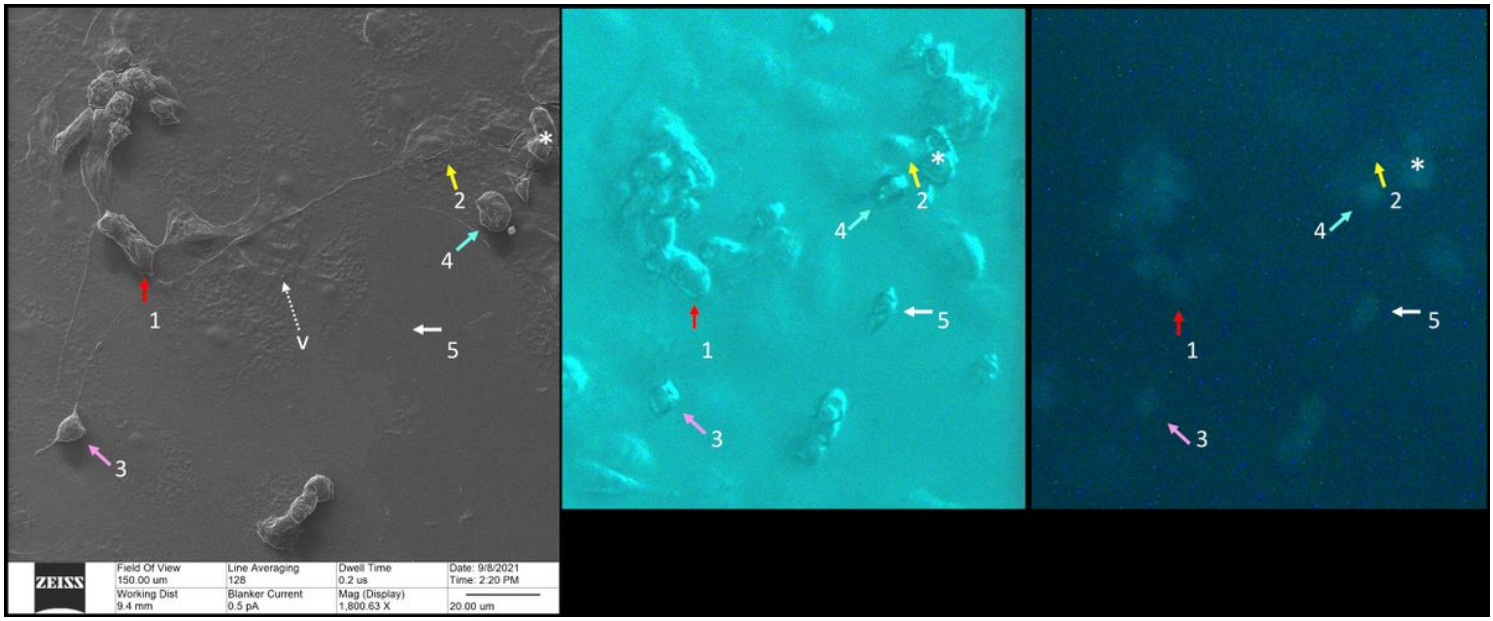

Figure 2

Correlative microscopy. A 150-micron square area shows two cells (1 and 2) connected by a TNT about 100 microns long. HeIM (left) shows the morphology of the cells, while green fluorescence microscopy provides data on their infectious status. HeIM shows a rounded bipolar cell (3) emitting TNT and being infected; it did not change its position regarding the prior acquired phase-contrast photomicrograph. Rounded infected cells tend to detach from the floor. Correlation between HeIM and Phase Contrast Microscopy shows that cell 4 changed its position slightly while cell 5 moved out of the field. HeIM picked the presence of vesicles in the area; the vesicle indicated by “v” in the figure (left) is magnified and shown in figure 9D. (HeIM 1,800 X; Optical Microscopy 400X).

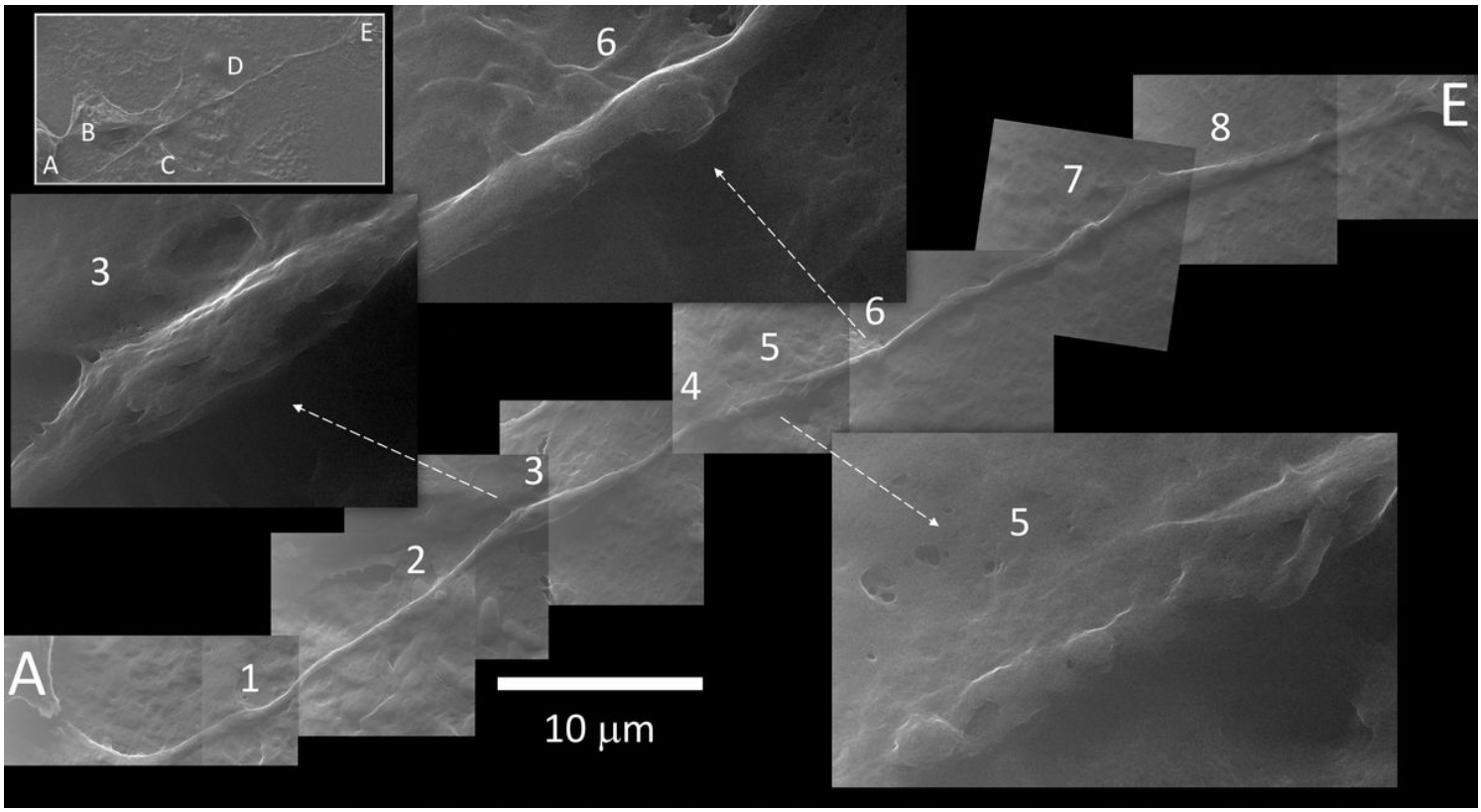

Figure 3

Tunneling Nanotube. The long TNT that connects cell A to B (named 1 and 2 in figure 2) interacts with at least three other cells along its path (B, C and D, in the top left inset). A mosaic reconstruction of HeIM micrographs (27,000X) highlights 8 notable events, some of which are magnified at a higher definition (54,000X). 1)-spherical bulging; 2)-well defined spherical bulging and membrane fusion, in a region rich in mitochondria; 3)-diameter enlargement by cargo content; 4)-spherical bulging close to a 5)-membrane fusion area; 6)-well defined spherical bulging; 7)-two close spherical bulging; 8)-diameter enlargement. Higher definition micrographs showed longitudinal cytoskeletal features under the membrane.

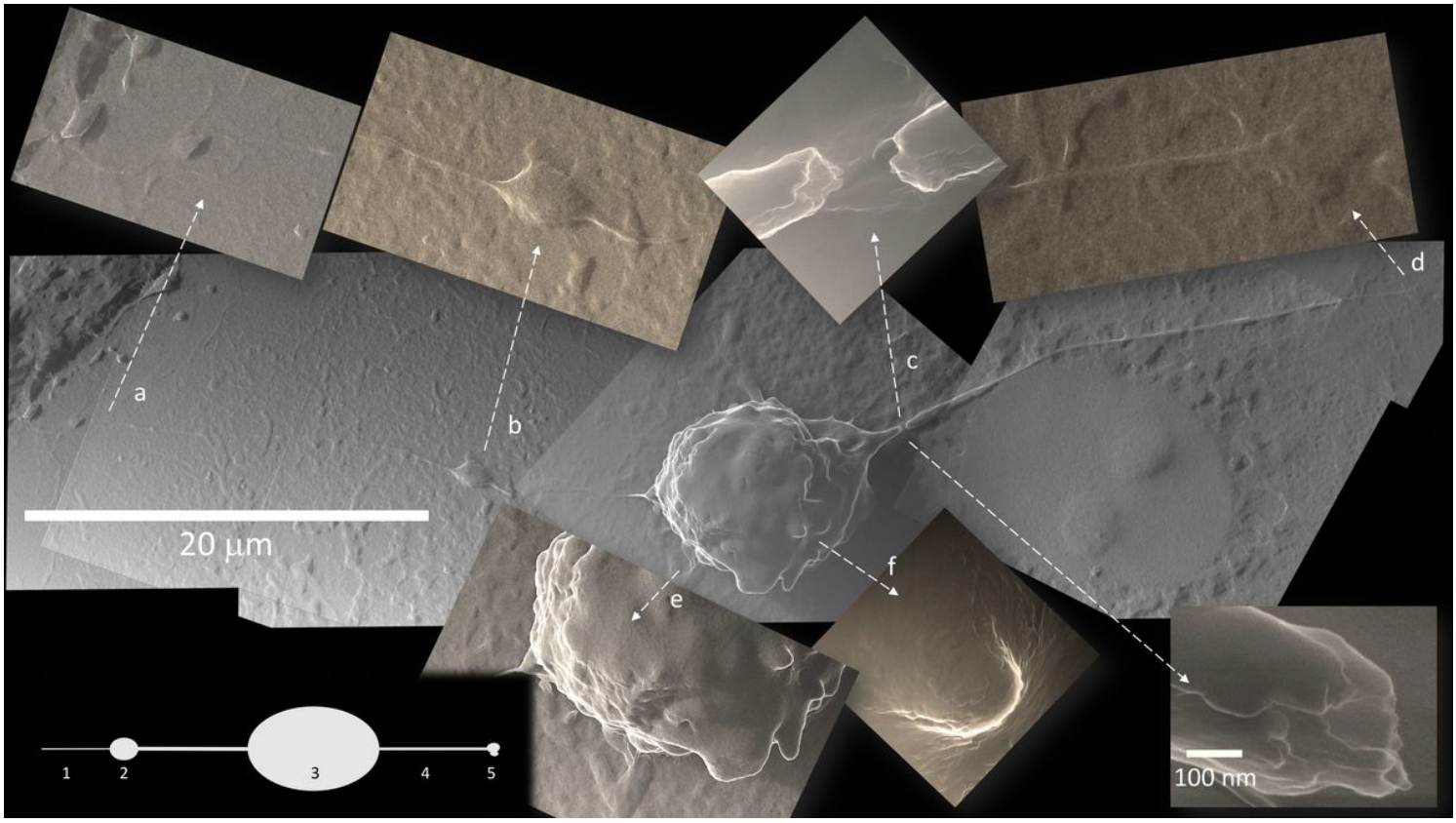

Figure 4

Details of a polarized infected cell. Cell #3 in figure 2 is visualized in a mosaic of photomicrographs taken at 27,000X.

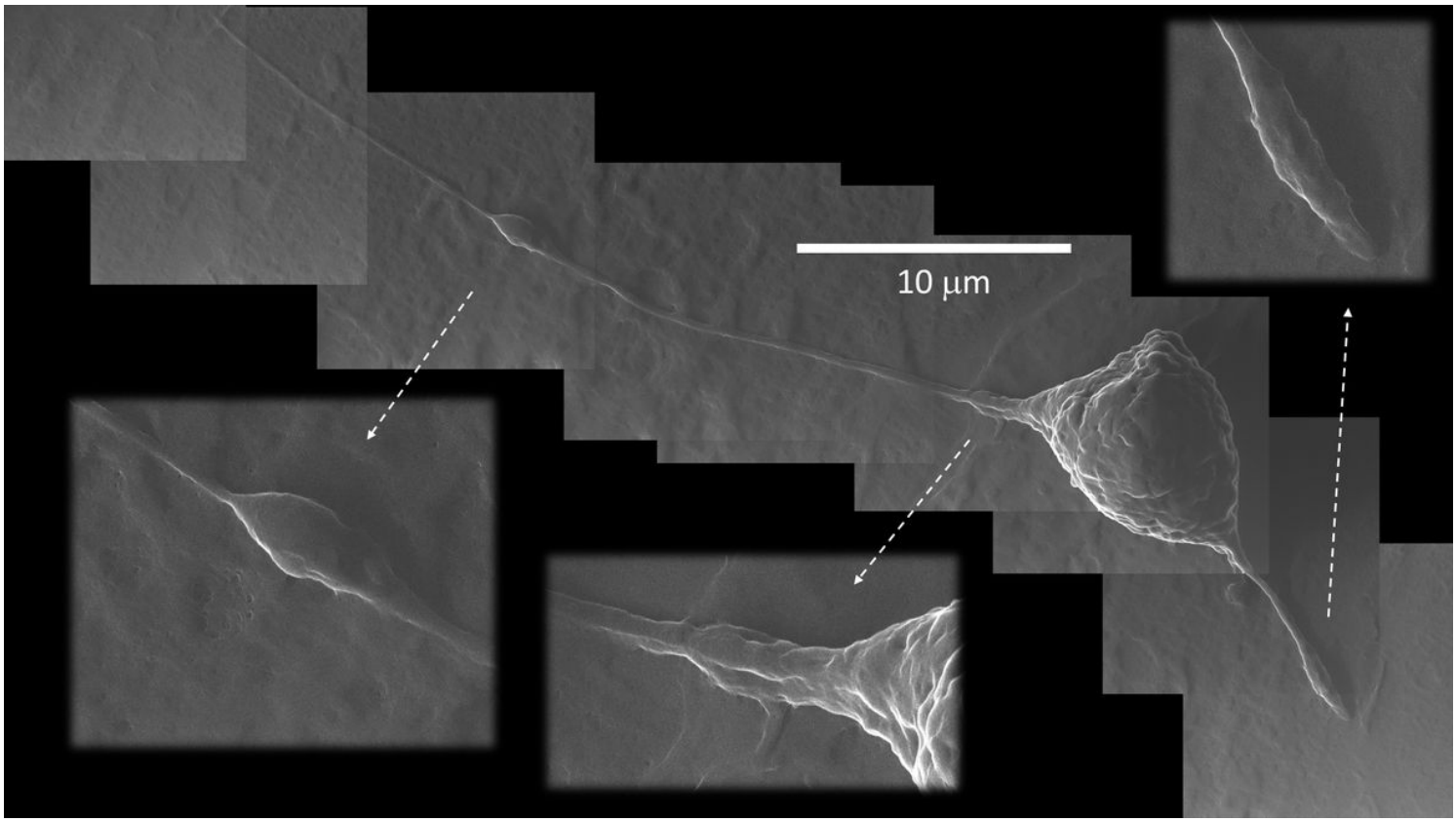

Figure 5

Details of a polarized infected cell. Cell #3 in figure 2 is visualized in a mosaic of photomicrographs taken at 27,000X.

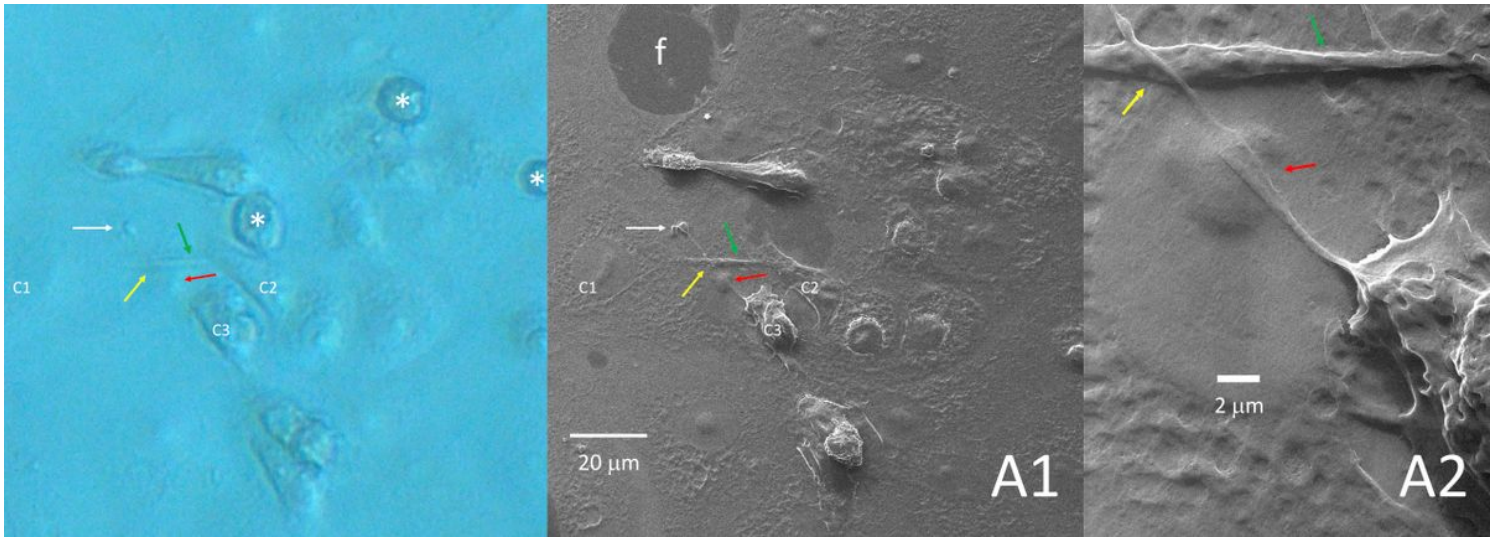

Figure 6

TNT overlap. An area of 130-micron square has been imaged (A1) that shows a TNE originating from cell C3 overlapping another TNT which connects cells C1 and C2 (green arrow). A region shows the bare floor of the culture well (f). TNT keep their individual structure when they cross each other (yellow arrow), but they may fuse their membrane when they overlap a cell (red arrow) (magnification in A2). The specific morphology often seen in a TNT polymorphic bulge termination is pointed by a white arrow. Correlation with a phase contract image taken before HeIM (left) shows three rounded infected cells detached from the floor (asterisks) that were no longer present in the subsequent HeIM photomicrograph.

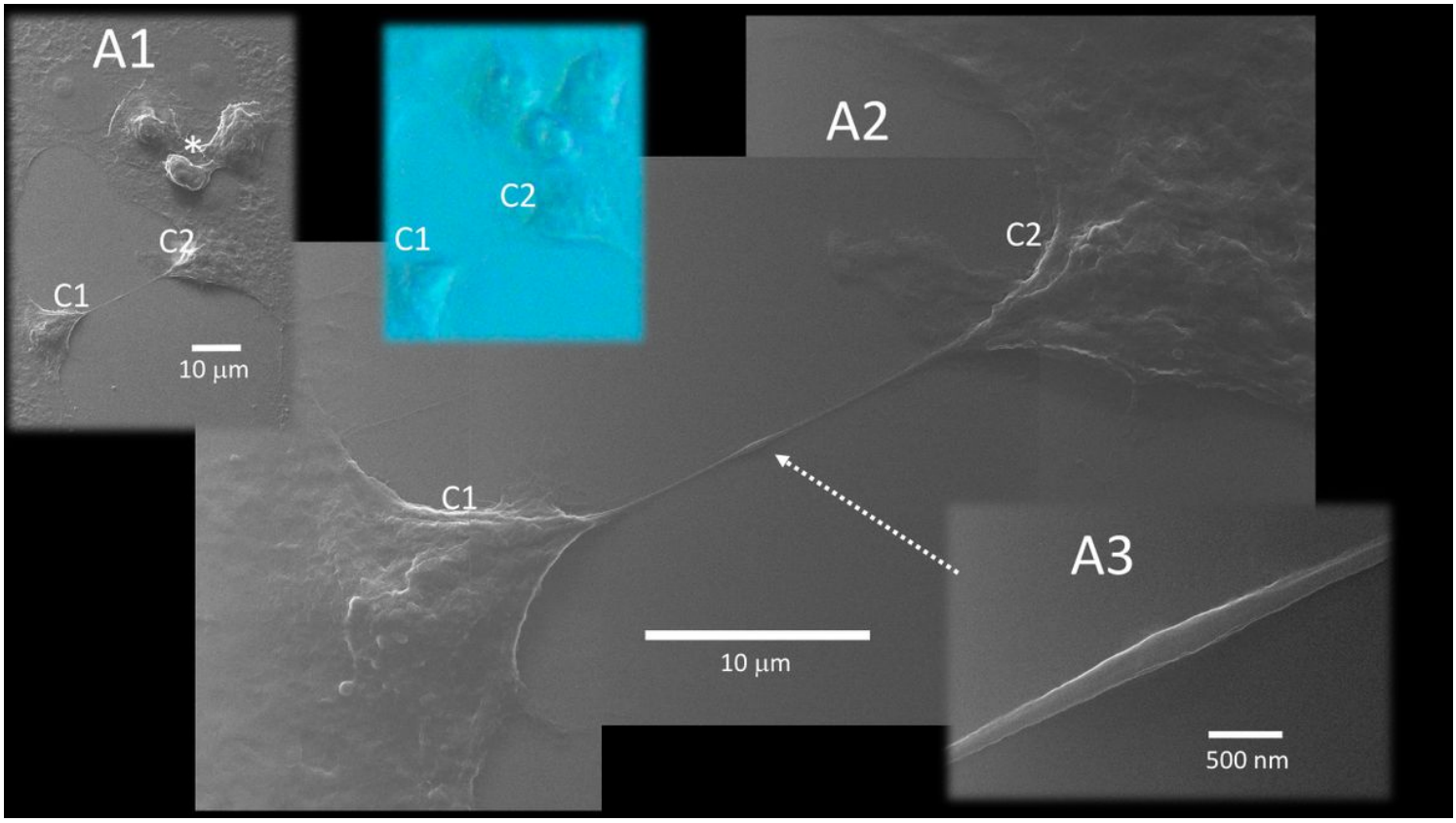

Figure 7

TNT stretched between two host cells. A TNT under mechanical tension between two cells (C1 and C2) lies on the well floor. Fully flat healthy cells and a trio of bulging and detaching infected cells (asterisk in A1) can be seen nearby. This stretched TNT pulls on both cells, shaping them with a stretched morphology (A2). We ruled out the possibility that this tension could be caused by the dehydration process because correlative microscopy showed the same stretched morphology in the hydration state in Phase Contrast prior to HeIM (blue inset). Stretched TNT between two cells often present a bulging mid-way (dotted arrow; magnification in A3). (magnification in A1 2,700X; in A2 10,800X; in A3 77,000)

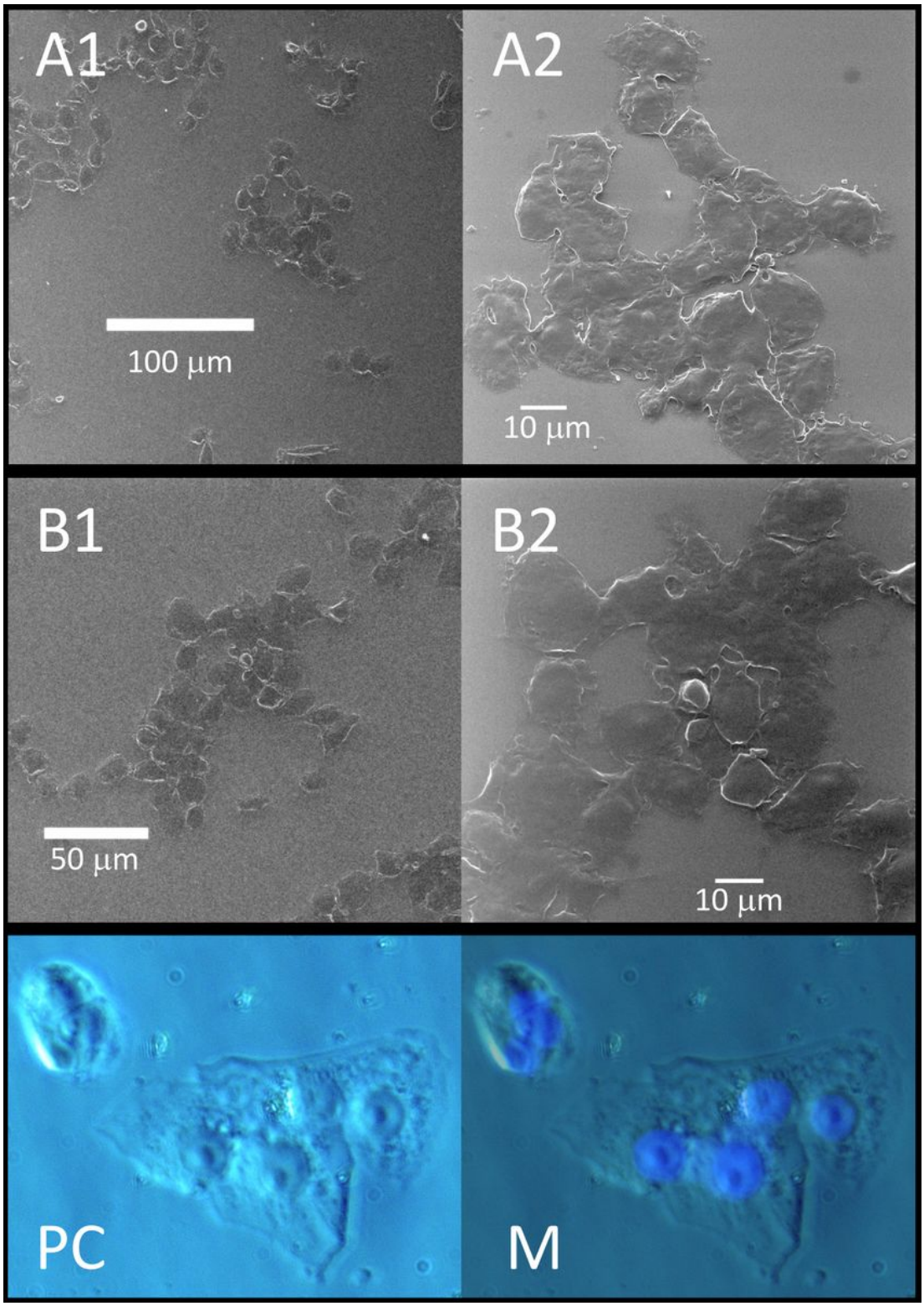

Figure 8

Fusion of SARS-CoV-2 infected host cells. Infected cells form submillimeter clusters of multiple fused cells at 24 hours post-infection. HeIM highlights the continuity of their membranes, while fluorescence microscopy shows the presence of multiple DAPI stained fluorescent nuclei (blue in M) in clusters of cells imaged with phase-contrast microscopy (PC).

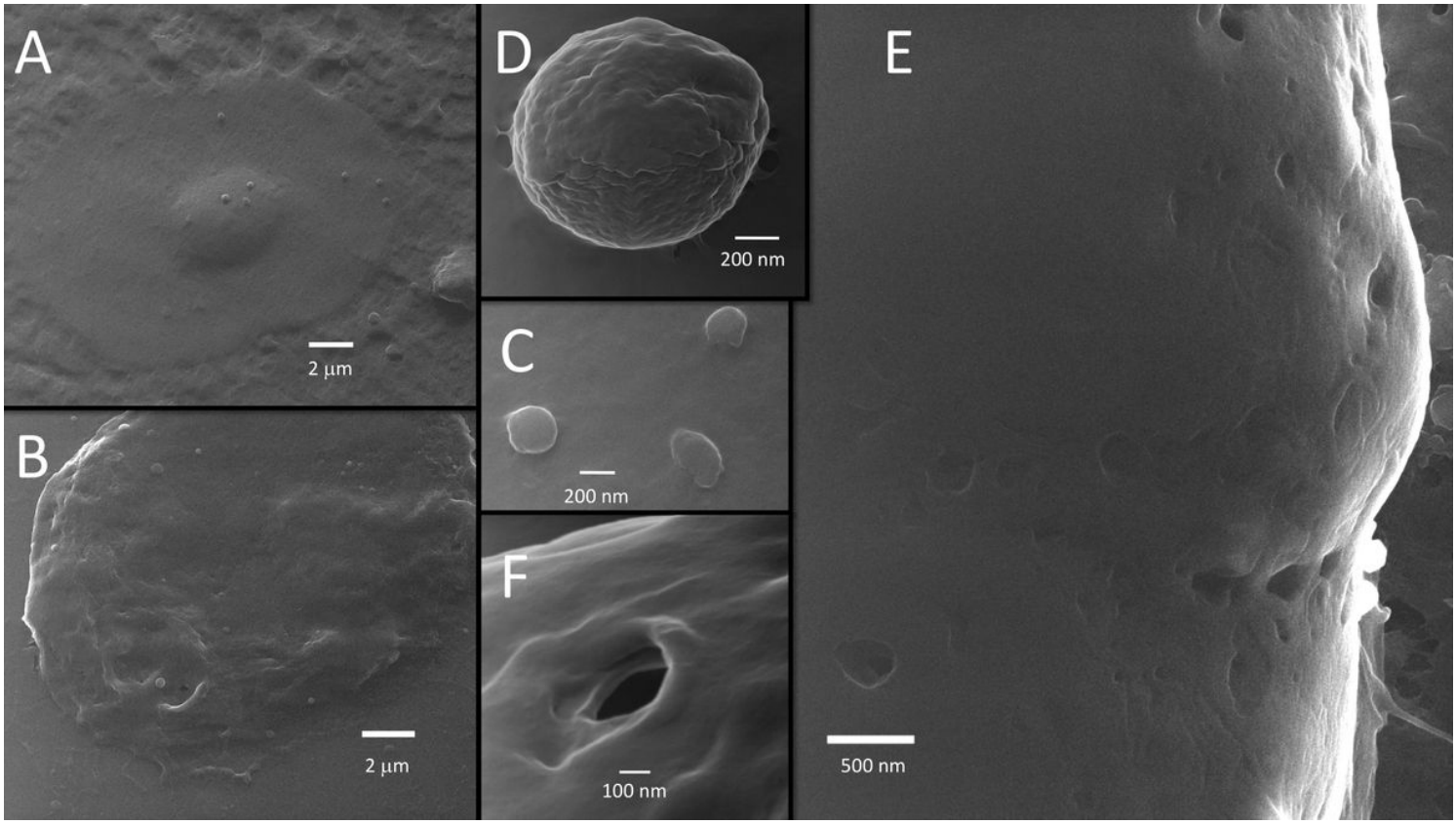

Figure 9

Vesicles and caveolae in SARS-CoV-2 infected host cells. Vesicles and caveolae are seen in infected cells. (magnification in A and B 10,800X; BC135,000X; D 180,000X; E 135,000X; F 270,000X)

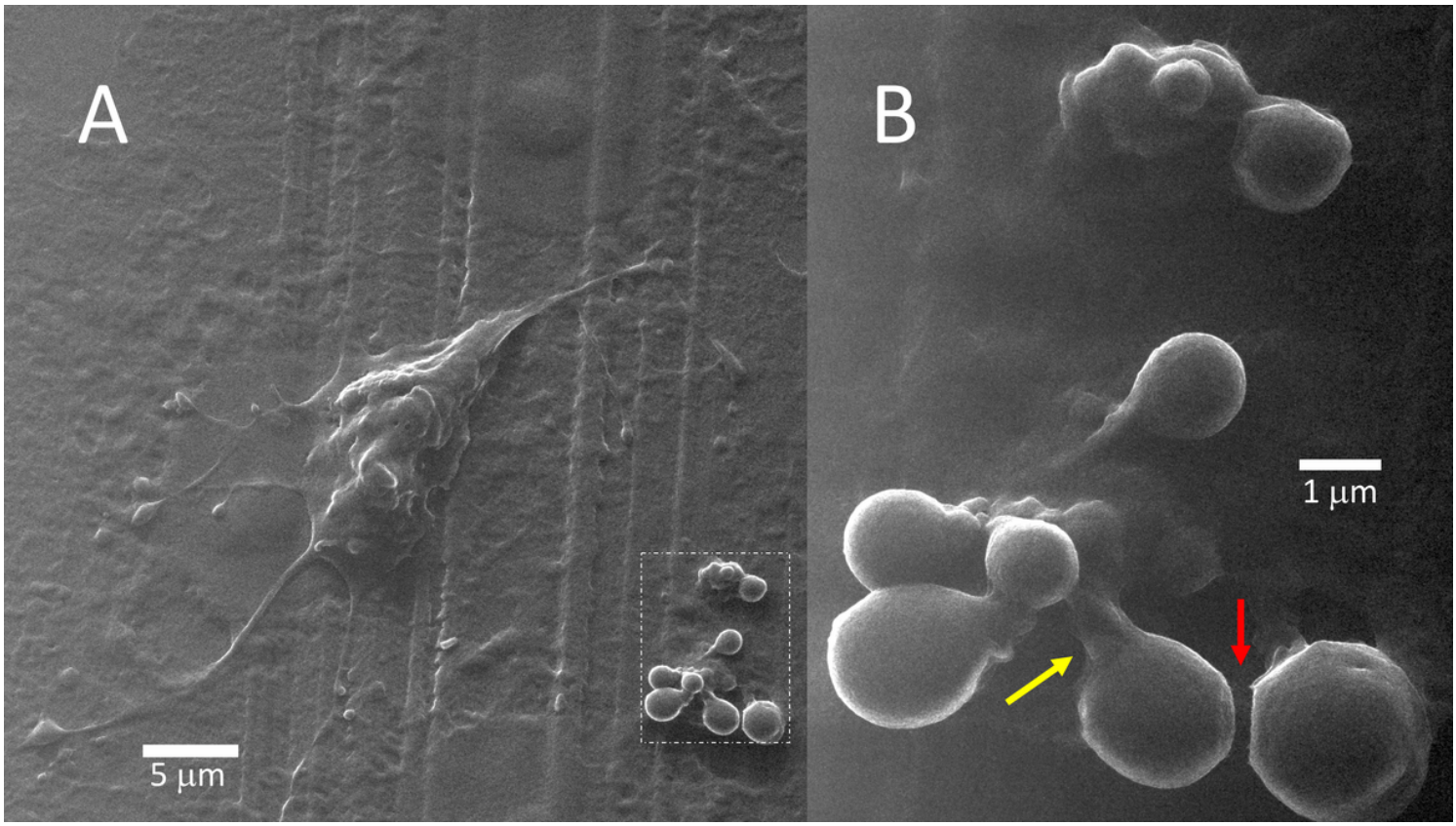

Figure 10

Apoptosis of SARS-CoV-2 infected host cell. Budding TNT with growth cones (A) may resemble budding apoptotic bodies captured just before leaving a disintegrating cell (B). Apoptotic bodies in B show a clear stalk (yellow arrow) and images suggesting a close membrane apposition (red arrow; detachment possibly due to dehydration). The parallel lines are the result of glass carving for reference frames. (magnification in A 5,400X; in B 27,000X)

Supplementary Files

This is a list of supplementary files associated with this preprint. Click to download.

- j11sNCfigbipolarcopy.jpg